Separability of wave solutions in nonlinear brass instrument modelling

Separability of wave solutions in nonlinear brass instrument modelling

R. L. Harrison-Harsley, and S. Bilbao

Citation: The Journal of the Acoustical Society of America **143**, 3654 (2018); doi: 10.1121/1.5043423
View online: https://doi.org/10.1121/1.5043423
View Table of Contents: http://asa.scitation.org/toc/jas/143/6
Published by the Acoustical Society of America

Separability of wave solutions in nonlinear brass instrument modelling (L)

R. L. Harrison-Harsley[a] and S. Bilbao
Acoustics and Audio Group, University of Edinburgh, Edinburgh, United Kingdom

(Received 19 March 2018; revised 31 May 2018; accepted 7 June 2018; published online 22 June 2018)

Travelling wave representations of wave propagation are commonly employed in brass instrument modeling and have been extended to the nonlinear regimes. For the case of a real brass instrument, the assumptions that lead to the travelling wave solutions no longer strictly hold. The validity of these assumptions is investigated here with regard to two typical parts of brass instrument geometry. The first example shows that there is a small interaction between forwards and backwards travelling waves in a cylindrical tube. The second example highlights nonlinear backscattering of a traveling wave caused by variations in the tube cross-sectional area.
 https://doi.org/10.1121/1.5043423

[AM] Pages: 3654–3657

I. INTRODUCTION

A physical description of a musical instrument relies crucially on nonlinear mechanisms. In the case of brass instruments, one is the well-known coupling mechanism between the lips and the instrument bore; another is the formation of shocks along the instrument bore, first observed by Hirschberg *et al.*[1] One underlying assumption is that, due to the high pass nature of the brass instrument bell, nonlinear propagation need only be considered in one direction—from the mouth of the player to the end of the instrument. The use of one-way wave equation models in brass instrument modeling is widespread.[2,3] However, it is clear that, due to variations in the bore cross-section, leading to incremental back-scattering along the length of the instrument, such a one-way model is incomplete, even in the linear regime. This short contribution is concerned with an examination of the validity of such one-way models.

II. MODEL

An acoustic tube may be characterised in terms of its cross-sectional area $S(z)$, which is a function of an axial coordinate z. A suitable nonlinear propagation model in such a tube of variable cross-section is the one-dimensional Euler system[4] that describes the time evolution of the pressure deviation p from atmospheric pressure P_0, particle velocity, $v(t, z)$ and density, $\rho(t, z)$, as functions of z and time, t. Prior to shock formation, the adiabatic assumption can be made, relating the total pressure $P = P_0 + p$ and density through the thermal coefficient, κ, and the ratio of specific heats, γ, so that $P = \kappa\rho^{\gamma}$, where $\kappa = P_0/\rho_0^{\gamma}$ and ρ_0 is the static air density. The Euler equations can then be expressed as the following two-variable system in p and v:

$$\partial_t p + v\partial_z p + \gamma(P_0 + p)\partial_z v + \gamma v(P_0 + p)\frac{\partial_z S}{S} = 0, \quad (1a)$$

$$\partial_t v + v\partial_z v + \kappa^{1/\gamma}(P_0 + p)^{-1/\gamma}\partial_z p = 0. \quad (1b)$$

Here, ∂_t and ∂_z indicate partial differentiation with respect to t and z, respectively. Under the adiabatic assumption, the local speed of sound c_{loc} is given as

$$c_{\text{loc}} = \sqrt{\gamma\kappa^{1/\gamma}(P_0 + p)^{(\gamma-1)/\gamma}}. \quad (2)$$

Equations (1a) and (1b) may then be rewritten as

$$(\partial_t + (v \pm c_{\text{loc}})\partial_z)\underbrace{\left(v \pm \frac{2}{\gamma - 1}c\right)}_{v_\pm} = \mp\frac{c_{\text{loc}} v\partial_z S}{S}, \quad (3)$$

where the local speed of sound is given in terms of a static part, c_0 (the linear speed of sound), and an oscillatory part, c, so that $c_{\text{loc}} = c_0 + c$. The wavelike variables $v_\pm$ are as indicated in Eq. (3) above so that $v_\pm \equiv v \pm [2/(\gamma - 1)]c$. Writing entirely in terms of the wavelike variables, Eq. (3) becomes

$$\left(\partial_t + \left(\pm c_0 + \frac{\gamma + 1}{4}v_\pm + \frac{3 - \gamma}{4}v_\mp\right)\partial_z\right)v_\pm = \mp\frac{\gamma - 1}{8}\frac{(v_+^2 - v_-^2)\partial_z S}{S}. \quad (4)$$

III. CYLINDER

Let us first consider the case of a cylinder, so that $\partial_z S = 0$. In this case, Eq. (3) becomes

$$(\partial_t + (v \pm c_{\text{loc}})\partial_z)v_\pm = 0. \quad (5)$$

The assumption that $v_- = 0$, so that only one wavelike solution (v_+) is present, implies that

$$c = \frac{\gamma - 1}{2}v = \frac{\gamma - 1}{4}v_+, \quad (6)$$

[a]Electronic mail: r.l.harrison-3@sms.ed.ac.uk

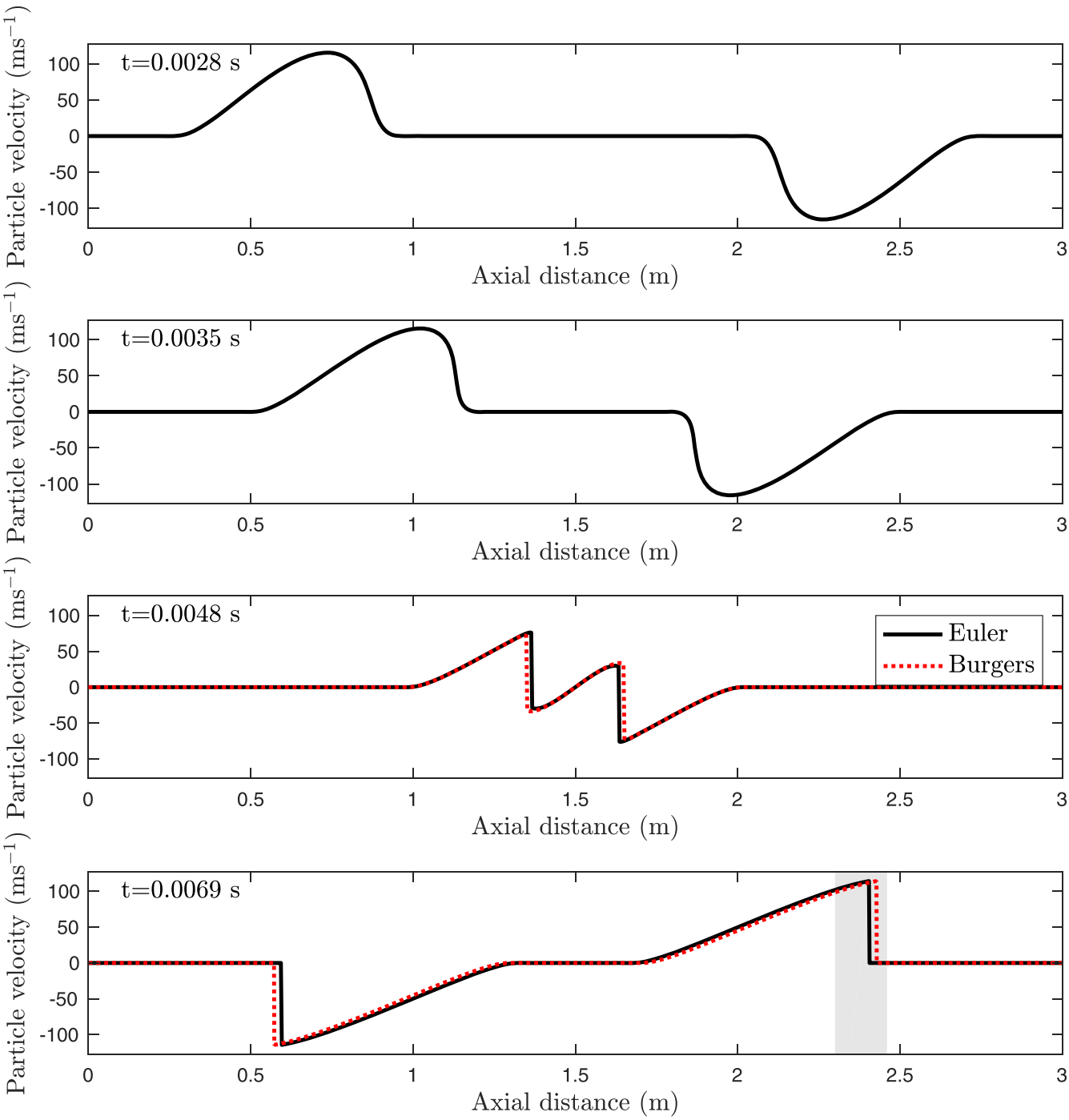

FIG. 1. (Color online) Time evolution of the particle velocity within a cylindrical acoustic tube excited at both ends with a Hann pulse at times as indicated, for the Euler equations (solid line) and Burgers equation (dotted line). Prior to the interaction, the two systems produce the same results, with discrepancies appearing after the interaction. The shaded region in the bottom frame is enhanced in Fig. 2.

which further implies that

$$\left(\partial_t + \left(\frac{1+\gamma}{4} v_+ + c_0\right)\partial_z\right) v_+ = 0. \tag{7}$$

Equation (7) is a Burgers equation with a linear advective term, and is used to model nonlinear propagation in a cylinder: in this case, a velocity wave v_+ travelling in the positive z direction. Provided that only one wave is present, the Burgers equation (7) provides the same solutions as the Euler equation (1): the solution (6) is derived under the assumption that there is no wave travelling in the opposite direction.

Wave propagation in brass instruments is bidirectional. In this case, one modeling approach is to make use of an uncoupled pair of equations[2,5] of the form of Eq. (7), in the two variables v_+ and v_-:

$$\left(\partial_t + \left(\frac{1+\gamma}{4} v_\pm \pm c_0\right)\partial_z\right) v_\pm = 0. \tag{8}$$

Each equation in Eq. (8) is derived under the assumption that the wave traveling in the opposite direction is zero—as

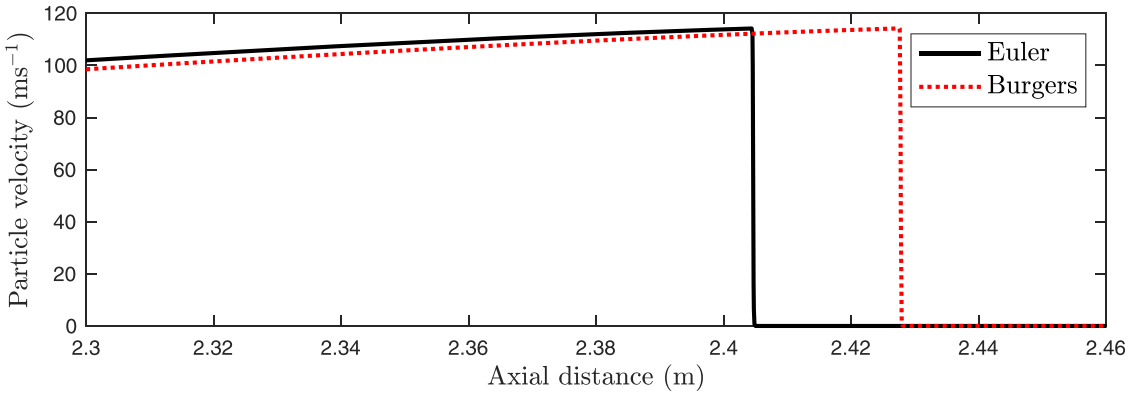

FIG. 2. (Color online) Enhanced view of forwards travelling waves in the shaded region of the bottom frame of Fig. 1. Solid line shows results from Euler equations, dotted line shows results from Burgers equation.

such, it does not follow from the physical system (3), which allows for pointwise interaction of the traveling waves everywhere along the bore.

Consider the scenario presented in Fig. 1: a cylindrical tube of length 3 m is excited at both ends by the same particle velocity signal but with opposite sign. Pulses travel from each end, with a period of overlap in the middle of the tube.

Simulations were performed at a sample rate of 10 MHz using a simple upwind finite-difference time-domain scheme for each model, given by Eqs. (4) and (8). In this case, we consider the air column within a cylinder excited by a velocity wave source at both ends by the same Hann pulse of duration 0.002 s and an amplitude of $c_0/3$. Although this driving amplitude is significantly higher than what would be present under real playing conditions, it is chosen to highlight the effect of interacting waves. A clear distinction between the two solutions is visible as a phase lag of the wavefronts of the solution to the Euler equations relative to those generated using the Burgers equation model. This is highlighted in Fig. 2, which focusses on the forwards travelling pulse from the bottom panel of Fig. 1. This lag in the solution to Euler equations is due to the reduced local speed of sound when the waves interact—this does not occur in the solutions to the Burgers equations. If excitation signals were of the same sign (not presented here), the solutions to the Euler equations would be ahead of those of the Burgers equations due to an increase in the local speed of sound.

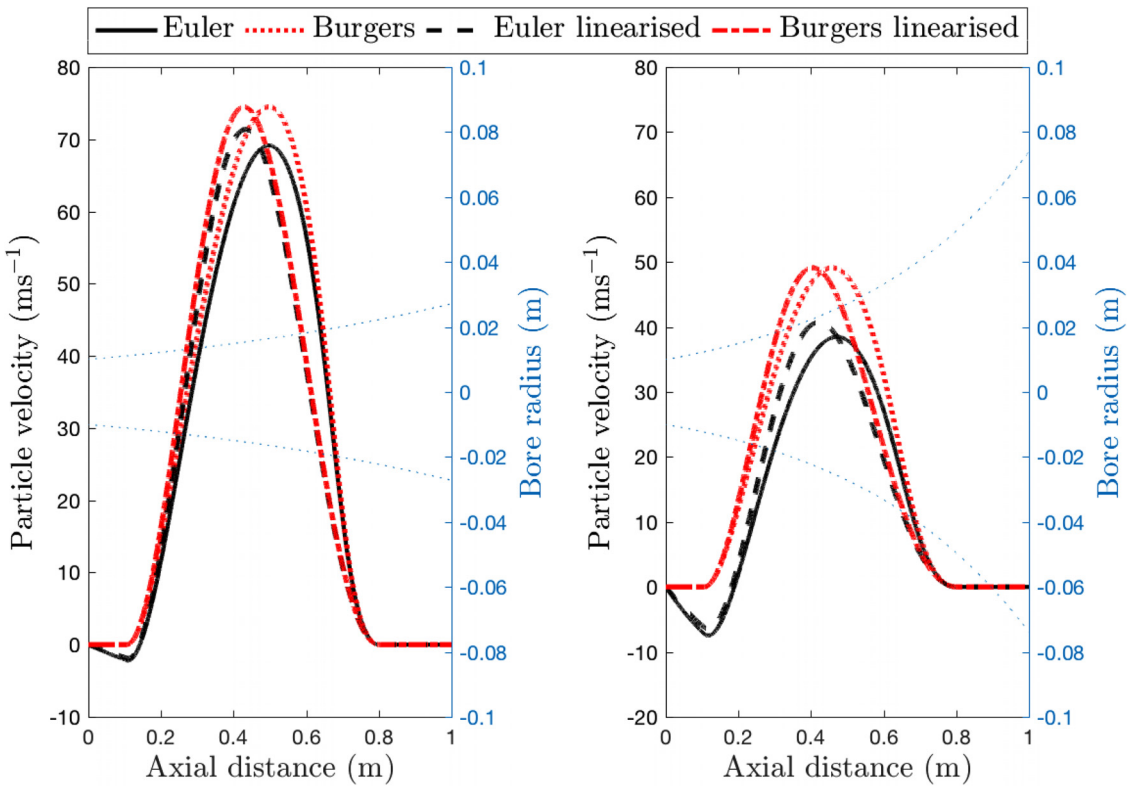

FIG. 3. (Color online) Snapshots of the particle velocity in two different exponential horns [area given by $S(z) = S_0 e^{\alpha x}$] simulated using different models: solid line, Euler equations; dotted line, Burgers equations; dashed line, linearised Euler equations (Websters' equation); dash-dot line, linearised Burgers equation. Left: $\alpha = 2\,\mathrm{m}^{-1}$. Right: $\alpha = 4\,\mathrm{m}^{-1}$. Bore profile is shown on second axis of each case.

IV. FLARING HORN

We now turn our attention to a spatially varying bore profile. The general model of wave propagation in such a tube is given by Eq. (3). In the case of a horn of slowly varying cross section, the right hand side can be assumed to be small, and some authors have extended the uncoupled model given in Eq. (8) to account for such variation as

$$\left(\partial_t + \left(\frac{1+\gamma}{4}v_+ + c_0\right)\partial_z\right)v_+ = -\frac{c_0 v_+ \partial_z S}{2S}, \tag{9a}$$

$$\left(\partial_t + \left(\frac{1+\gamma}{4}v_- - c_0\right)\partial_z\right)v_- = \frac{c_0 v_- \partial_z S}{2S}. \tag{9b}$$

This equation is the form used by Berjamin *et al.* for trumpet modelling. At this point, it is important to note that the pair of uncoupled one-way advection equations above does not reduce, in the linear case, to the equations describing the dynamics of an acoustic tube. In particular, they cannot recombine to yield Webster's equation. An easy way to see this is to examine Eq. (9) under linear conditions, and using the scaled variables $\tilde{v}_\pm = \sqrt{S}v_\pm$, in which case one arrives at

$$(\partial_t \pm c_0\partial_z)\tilde{v}_\pm = 0. \tag{10}$$

Thus, although gross effects of amplitude scaling of a wave due to variations in cross section are accounted for in model (9), there are no effects of scattering within the tube. A more important conclusion, in the context of brass instrument modeling, is that the instrument resonances will be unaffected by the bore profile S which, indeed, does not appear in Eq. (10). One may conclude that such a model is of dubious utility in the modeling of brass instruments of variable cross section.

In the nonlinear case, other effects emerge; simulation results comparing Eq. (9) and the Euler equations (4), along with their linearised forms, are shown in Fig. 3, where simulations are performed at 10 MHz. In this case, an exponential horn is used as the bore profile, defined by

$$S(z) = \pi 0.01^2 e^{\alpha z}, \tag{11}$$

where α is the flaring constant. The narrow end of the horn is excited with the same velocity source used in Sec. III. For $\alpha = 2\,\mathrm{m}^{-1}$, scattering is observed for the Euler equation and its linearised form, which is not present for the one-way velocity equations, as seen in the negative tail of the pulse. This scattering is even more extreme for $\alpha = 4\,\mathrm{m}^{-1}$. In addition, the amplitude of the wave is larger for the simulation using the Burgers equation and its linearised form. In the linear case, this larger amplitude does not affect the frequency content of the pulse. However, in the nonlinear case, the larger amplitude of the wave increases the nonlinearity, thus causing a greater wave steepening to occur in this region.

V. CONCLUSION

Unidirectional Burgers models of wave propagation in acoustic tubes allow for a convenient analysis of high amplitude playing in brass instruments. And yet, the strong underpinning assumption of separability conflicts with accepted models of wave propagation in tubes of variable cross section; the validity of such an assumption has been examined here.

It is clear that the assumption is nearly valid for tubes of cylindrical cross section, as described in Sec. III; there is a small interaction effect for very high amplitude wave propagation, leading to a slight change in the overall wave speed during the interaction itself. Some further research, advancing on the experiments by Menguy and Gilbert,[6] would be needed to determine the cumulative effect of this interaction. The results for wave propagation in a horn of variable cross section, as described in Sec. IV, show a more pronounced difference between the two models than in the case of the cylinder. The most prominent difference between the two models is the absence of scattering in the Burgers model. This effect is particularly important for brass instruments, as the flaring portion of the bell modifies the lower resonance of the instrument, which are crucial in terms of the musical characterisation of the instrument and its playability. Simulations using the Burgers equation (9) for a spatially varying horn result in an instrument with the same resonances as a cylindrical tube of equal length.

ACKNOWLEDGMENTS

This research was supported by the European Research Council, under Grant No. ERC-2011-StG-279068-NESS.

[1] A. Hirschberg, J. Gilbert, R. Msallam, and A. P. J. Wijnands, "Shock waves in trombones," J. Acoust. Soc. Am. **99**(3), 1754–1758 (1996).

[2] H. Berjamin, B. Lombard, C. Vergez, and E. Cottanceau, "Time-domain numerical modeling of brass instruments including nonlinear wave propagation, viscothermal losses, and lips vibration," Acta Acust. united Acust. **103**, 117–131 (2017).

[3] S. Maugeais and J. Gilbert, "Nonlinear acoustic propagation applied to brassiness studies, a new simulation tool in the time domain," Acta Acust. united Acust. **103**, 67–79 (2017).

[4] P. G. LeFloch and M. Westdickenberg, "Finite energy solutions to the isentropic Euler equations with geometric effects," J. Math. Pures Appl. **88**(2), 389–429 (2007).

[5] R. Msallam, S. Dequidt, R. Caussé, and S. Tassart, "Physical model of the trombone including nonlinear effects. Application to the sound synthesis of loud tones," Acust. Acta Acust. **86**, 725–736 (2000).

[6] L. Menguy and J. Gilbert, "Weakly nonlinear gas oscillations in air-filled tubes; solutions and experiments," Acust. Acta Acust. **86**, 798–810 (2000).